8-2009

Purification and Thermodynamic Analysis of The Stability of HIV-1 Reverse Transcriptase in the Presence of Efavirenz

Chantal A. SanMiguel

Purification and Thermodynamic Analysis of The Stability of HIV-1 Reverse Transcriptase in the Presence of Efavirenz

---

by Chantal A. SanMiguel

Undergraduate Honors Thesis

Directed by

Dr. Vince J. LiCata
Lewis S. Flowers Professor
Brij Mohan Distinguished Professor
Department of Biological Sciences

Submitted to the LSU Honors College in partial fulfillment of the Upper Division Honors Program

August 2009

Louisiana State University and Agricultural & Mechanical College
Baton Rouge, Louisiana

Table of Contents

I. Abstract

A member of the Pol I family of polymerases, Human Immunodeficiency Virus reverse transcriptase (HIV-RT) replicates the HIV-1 viral genome. The hand-shaped enzyme facilitates HIV-1 propagation in the human host and is consequently a primary target for antiretroviral drugs. In this study, HIV-RT was expressed and purified to homogeneity using a previously published protocol. The purified protein was then structurally and thermodynamically analyzed by circular dichroism (CD) spectroscopy and thermal denaturation. The HIV-RT CD spectrum shows it to be folded following purification. Thermal denaturation of HIV-RT yielded a two-state melting curve that fit the van't Hoff equation and reported a melting temperature (Tm) of 48.3 °C and a ΔH^{app} of 84.2 kcal/mol. In addition to CD spectroscopy, a nucleotide incorporation assay was used to monitor the thermal stability of HIV-RT in the presence and absence of 1 uM efavirenz. In this assay, the residual nucleotide incorporation activity remaining after incubation of the protein at different temperatures is used as a measure of protein unfolding. The Tm of the apo-protein in the nucleotide incorporation assay approach was found to be equal to the Tm generated from the thermal denaturation of HIV-RT by CD spectroscopy. When exposed to the drug, HIV-RT exhibited a Tm that was not significantly different from that of apo-protein. Neither the drug binding energy nor the previously-reported, enhanced dimerization effect of efavirenz were reflected in a shift in Tm but it was evident in an 8.2 kcal/mol enhancement of the ΔH^{app} that correlates with the expected energy of the binding of efavirenz. Since major pharmaceutical companies are increasingly using Tm in the drug-screening process, this study demonstrates the importance of considering multiple criteria before discounting the effectiveness of certain compounds.

II. Introduction

Structure and Function of HIV-1 Reverse Transcriptase

A major drug target for a number of globally-prescribed antiretroviral medications, HIV-1 reverse transcriptase (HIV-RT) is required for viral replication and disease progression [1]. HIV-RT catalyzes DNA polymerization, copying genomic, single stranded RNA into single stranded DNA, and using either an RNA or a DNA template. This new, single-stranded DNA is then converted into double-stranded, proviral DNA that can be incorporated into the host's genome, allowing for viral propagation. Non-nucleoside reverse transcriptase inhibitors (NNRTIs) slow the DNA polymerization activity of HIV-RT dramatically. However, the precise mechanism by which NNRTIs interact with HIV-RT and reduce its ability to function is not completely understood. A more extensive understanding of the biophysical interactions between these drugs and their target protein is essential to the improvement of current antiretroviral medications and to the development of novel inhibitors.

Consisting of 51 kDa (p51) and 66 kDa (p66) subunits, HIV reverse transcriptase exhibits the highest stability and biological activity in its p51/ p66 heterodimeric form [2]. By cleaving the p66 polypeptide between Tyr441 and Phe440, viral protease removes the ribonuclease H (RNase H) subdomain (see Figure 2) and produces p51 [3]. The p51 and p66 subunits, shown in Figure 1, have similar hand-like structural organizations, including finger, palm and thumb domains. Both the p51 and p66 subunits share a fourth pol subdomain, termed the "connection" region, as it separates the thumb and RNase H subdomains from the rest of the structure in p66 [4].

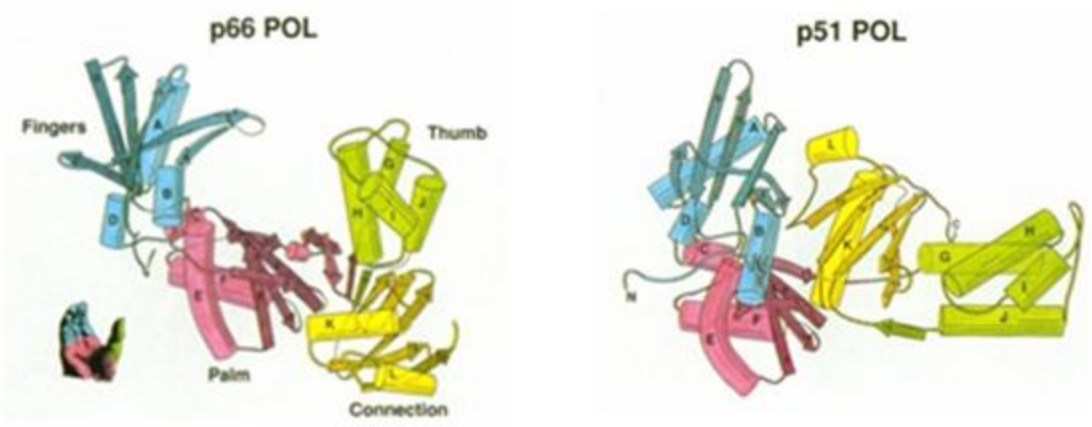

Figure 1. Polymerase domains of the p66 and p51 subunits of HIV-RT, demonstrating the different conformations of the finger (blue), palm (pink), connection (yellow) and thumb (green) subdomains. This figure is taken from Jacobo-Molina et al, Figures 2A and 2B [5].

Although the two subunits of HIV-RT have identical amino acid sequences, except for the removal of RNase H, their conformations are dissimilar and the p51 subunit does not have a distinct cleft [5].

The unique structures of the p51 and p66 subunits confer different functional roles. HIV-RT is a multifunctional enzyme, exhibiting RNase H activity as well as RNA and DNA-dependent polymerase functions (Figure 2), [6]. Since the polymerase and RNase H active sites of the HIV reverse transcriptase are located on p66, p51 is thought to serve a primarily structural role [8]. However, Steitz has deduced that the tRNA primer binding site and a segment of the template-primer binding site are located on the p51 subunit [5].

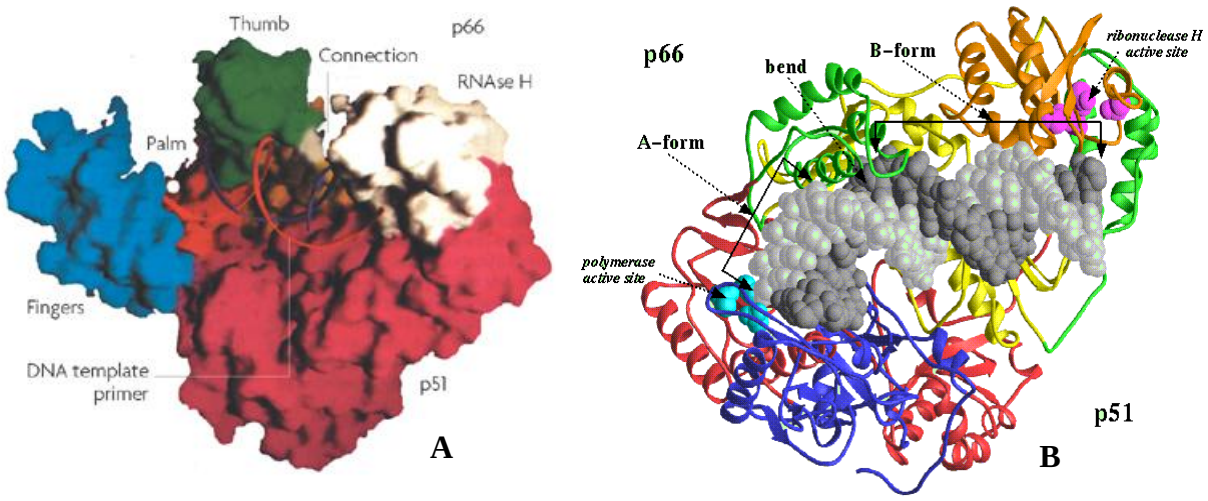

Figure 2. **A.** Space-filling view of the structure of HIV RT, showing finger, palm, thumb and connection domains. By cleaving the p66 polypeptide between Tyr441 and Phe440, viral protease actually produces p51 [3]. This figure is taken from Tantillo et al, Figure 2 [2]. **B.** Ribbon diagram view of the structure of HIV-RT/dsDNA. Protein-nucleic acid interactions occur primarily within the thumb, palm and finger domains of the p66 subunit. As shown above, the template-primer demonstrates A-form and B-form regions, with a 40-45 degree bend in between [5]. This figure is taken from Das et al, Figure 2 [7].

The asymmetry of HIV-RT is clearly apparent in the crystal structure of the protein (Figure 3). The two subunits of the dimer are asymmetrically oriented relative to one another. The palm region of p51 is translated 16 Å and rotated 74° in relation to the palm domain of p66 [5]. In effect, the HIV-RT subunits exhibit a roughly "head to tail" arrangement and the majority of intersubunit interactions take place in three specific locations. P51 and p66 predominately interact at the interface of their "connection" subdomains [5]. Noncovalent linkages between the subunits also occur between the end of the p51 thumb and the p66 RNase H domain as well as between p66 palm region and the end of the p51 fingers [5].

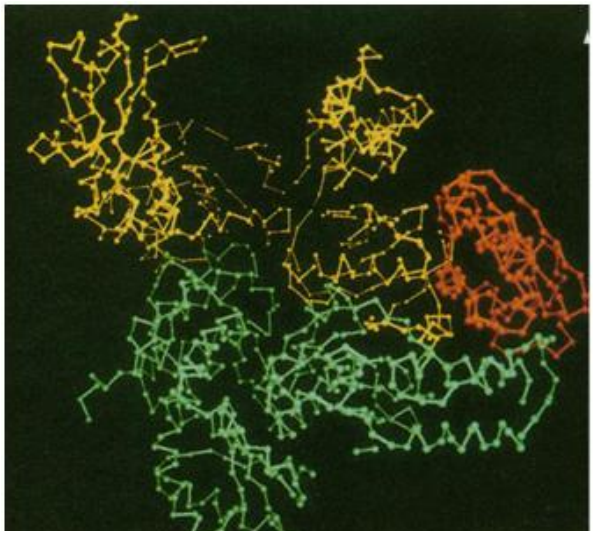

Figure 3. Crystal Structure of the HIV-RT heterodimer, showing the "head-to-tail" orientation of the p51 and p66 subunits [5]. The larger, p66 subunit is colored yellow and its RNase H domain is shown in orange. Smaller and lacking an RNase H domain, the p51 subunit is shown in green. This figure is taken from Jacobo-Molina et al, Figure 3A [5].

HIV-RT exhibits both structural and functional commonality with Klenow and Klentaq polymerases (Figure 4). Steitz and associates has identified direct similarities in the palm domains of p66 and Klenow [10]. The crystal structure of p66 shares a striking resemblance to that of Klenow (Figure 5). If the α-carbon backbones of the palm subdomains of the two polymerases are 3 dimensionally aligned, the catalytically important Asp^{185}, Asp^{186}, and Asp^{110} residues of HIV-RT overlap the active Asp^{882}, Glu^{883}, and Asp^{710} residues of Klenow. This commonality may additionally account for the similar catalytic behavior of HIV-RT and Klenow, yet it does not explain its behavior during heating.

In this study, the dimeric HIV-RT protein was expressed and purified following a procedure developed by Le Grice and associates [9]. The purification procedure consisted of a series of three columns (Nickel, Heparin and UNO-Sphere). In between columns, the fractions collected were analyzed by SDS-PAGE and elution profiles were generated. Following the purification of HIV-1 reverse transcriptase, a series of biophysical studies was performed in order to better understand the properties of the protein. HIV-1 reverse transcriptase was concentrated and evaluated by circular dichroism (CD) spectroscopy.

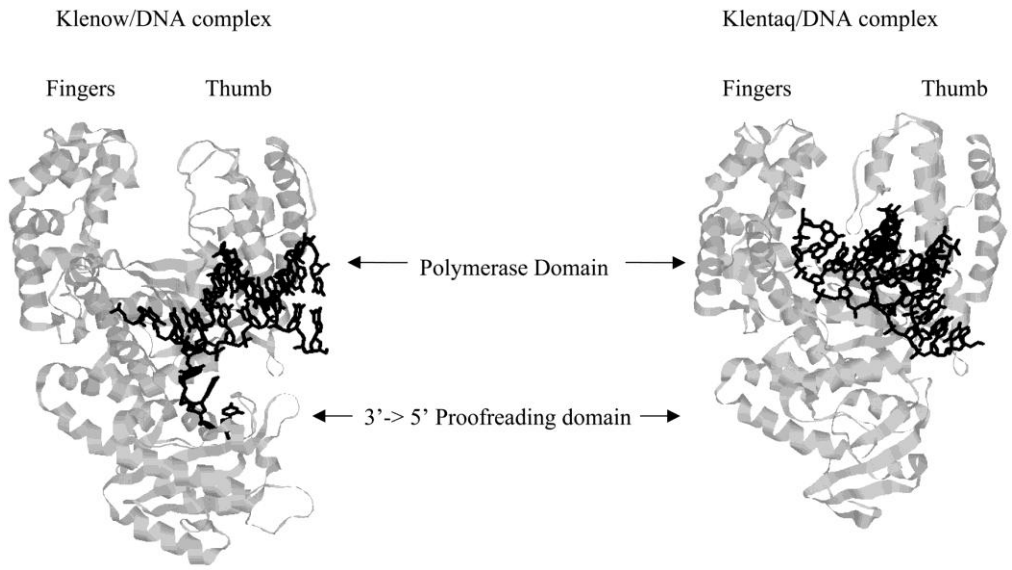

Figure 4. Crystal Structures of the Klenow/DNA complex (1KLN) and the Klentaq/DNA complex (4KTQ). This figure demonstrates the similarity between the two enzymes; however, Klenow possesses 3' - 5' proofreading, exonuclease activity that is absent in Klentaq. This figure is taken from LiCata and associates, Figure 1 [20].

Following a thermodynamic analysis of the folding of HIV-RT itself, the primary objective of this project was to investigate the effect of currently-prescribed antiretroviral medications on the interaction of the p51 and p66 HIV reverse transcriptase subunits. Specifically targeting HIV-RT, non-nucleoside reverse transcriptase inhibitors (NNRTIs) bind to the protein and inhibit the polymerization action of the protein (Figure 6).

NNRTIs induce a conformational change in the active site and reduce the nucleoside binding affinity of its residues, slowing DNA synthesis via noncompetitive inhibition [12]. While some preliminary research has been done on the effect of NNRTIs on

HIV-RT dimerization, a quantitative thermodynamic analysis has yet to be used to analyze the effect of these drugs. Barkley and Tachedjian have independently proposed that efavirenz, an NNRTI, can enhance interactions between the subunits of HIV-RT [14, 15]. Efavirenz, also known as Sustiva® or Stocrin®, is a frequently-prescribed NNRTI (Figure 8). It was approved by the FDA in 1998 and it is strictly used in combination therapy, or drug cocktail regimens [23].

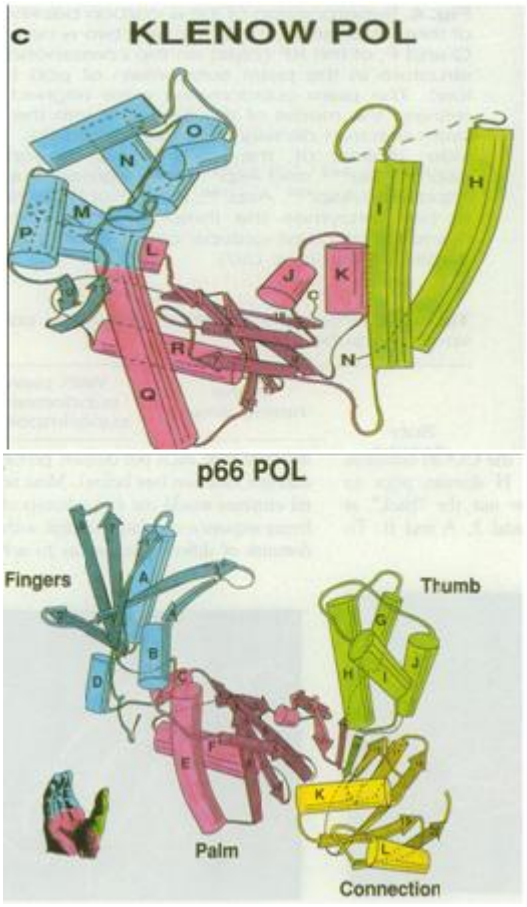

Figure 6. Crystal structures of the p66 subunit of HIV-RT and Klenow polymerase. The palm subdomains of the two proteins are similarly oriented. Although the palm domains of HIV-RT and Klenow appear the same, the polymerases have structurally different finger domains. While the finger domain of Klenow is predominately alpha-helical, HIV-RT's finger domain is a has areas consisting of beta sheets. This figure was taken from Steitz and associates [10].

This study was designed to further evaluate Barkley and Tachedjian and associates' hypothesis and to investigate the effects of efavirenz on the binding affinity of p51 and p66 using the methods and principals of protein unfolding. HIV-RT was purified in-house and optically analyzed by CD spectroscopy. This technique was then

used to melt the protein in its native state and, when fitted to the van't Hoff equation, to determine a Tm and ΔH^{app} for apo-HIV-RT.

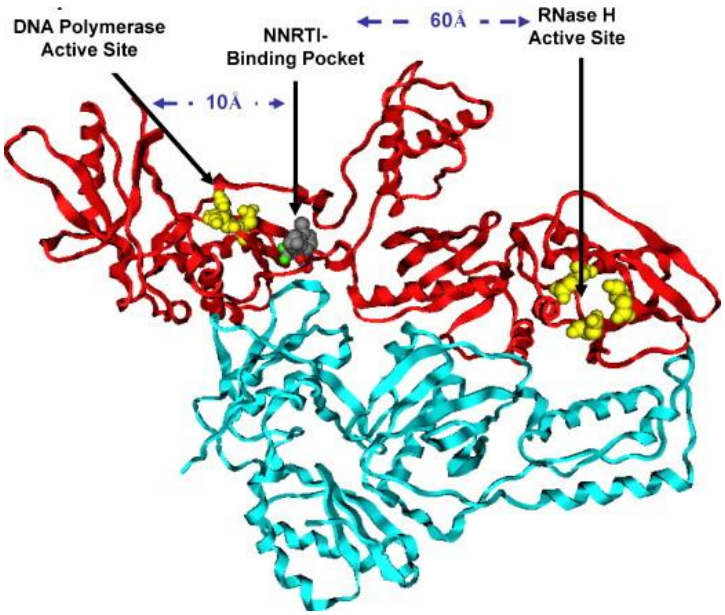

Figure 7. Ribbon diagram, showing HIV-RT in complex with efavirenz, also known as Sustiva, Stocrin, or $C_{14}H_9ClF_3NO_2$ (PDB 1FK9). Residues located in the DNA polymerase active site (Asp110, Asp185, Asp186) and the RNase H active site (Glu478, Asp443, Asp498) are indicated with yellow spheres. This figure was taken from Tachedjian et al, Figure 3 [13].NNRTIs function allosterically, binding to a hydrophobic region on the palm subdomain of the p66 subunit that is distinct from the active site (Figure 8).

Nucleotide incorporation was used in this study to monitor the thermal stability of efavirenz-bound HIV-RT and apo-HIV-RT. The Tm's yielded by native protein both techniques were compared in order to assess the validity of using nucleotide incorporation as a measure of HIV-RT unfolding.

A major dilemma in further HIV drug development, the frequent evolution of drug resistant viral strains, continues to present the necessity for the development of novel inhibitors. This study comparatively investigates the stability HIV-RT following exposure to

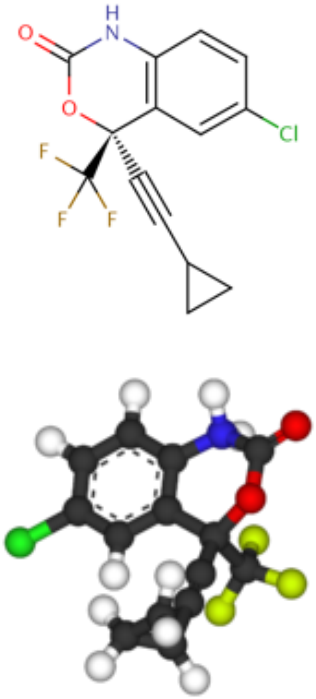

Figure 8. Molecular structure of efavirenz. This figure was taken from the DrugBank website listing for efavirenz . Efavirenz, $C_{14}H_9ClF_3NO_2$, also known as Sustiva® or Stocrin®, is an NNRTI that is frequently prescribed in highly active antiretroviral therapy (HAART), along with lamivudine and zidovudine or tenofovir [16].

efavirenz with the hope of contributing to our understanding of current antiretroviral medications.

An increased knowledge of the interaction between NNRTIs and HIV-RT could be beneficial to drug development. Hopefully, the biophysical information generated during this project may be useful provide drug developers with information helpful in the modification of improved NNRTIs. Thus, a better understanding of interaction between p51 and p66 could eventually lead to the production of novel HIV-RT dimerization inhibitors.

II. Materials and Methods

A. Purification of HIV-RT

HIV-RT was expressed and purified to homogeneity by following a protocol adapted from the LeGrice and associates (see Appendix A for purification protocol). Major alterations to the LeGrice protocol included a stepwise elution method and a larger starting culture volume. A recombinant, polyhistidine (His) tagged HIV-RT expression clone (p6H RT-PR), obtained from the LeGrice laboratory, was expressed in *E. coli* (Figure 10).

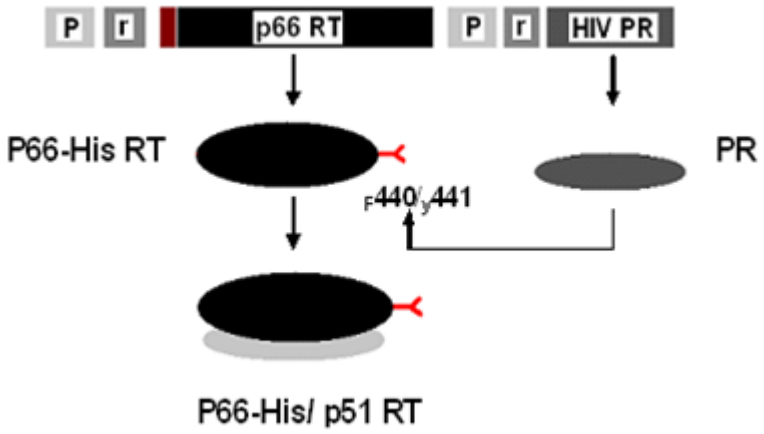

Figure 9. Expression of the p6H RT-PR clone in *E. coli.* The recombinant plasmid prepared by the LeGrice lab expressed both His-tagged, heterodimeric p51/p66 HIV-RT as well as HIV protease (PR). PR cleaves the p66 subunit of HIV-RT between Tyr-441 and Phe-440, producing the smaller p51 subunit. The repressible promoter (p) and synthetic ribosome binding site (r) are also shown on the expression cassette figure. The portion of the RT coding sequence that generates the 6 histidine extension is maroon. LeGrice and associates engineered the coding sequence to yield HIV-RT with C terminus His-tagged p66. This figure was adapted from Figure 1 from LeGrice and associates [9].

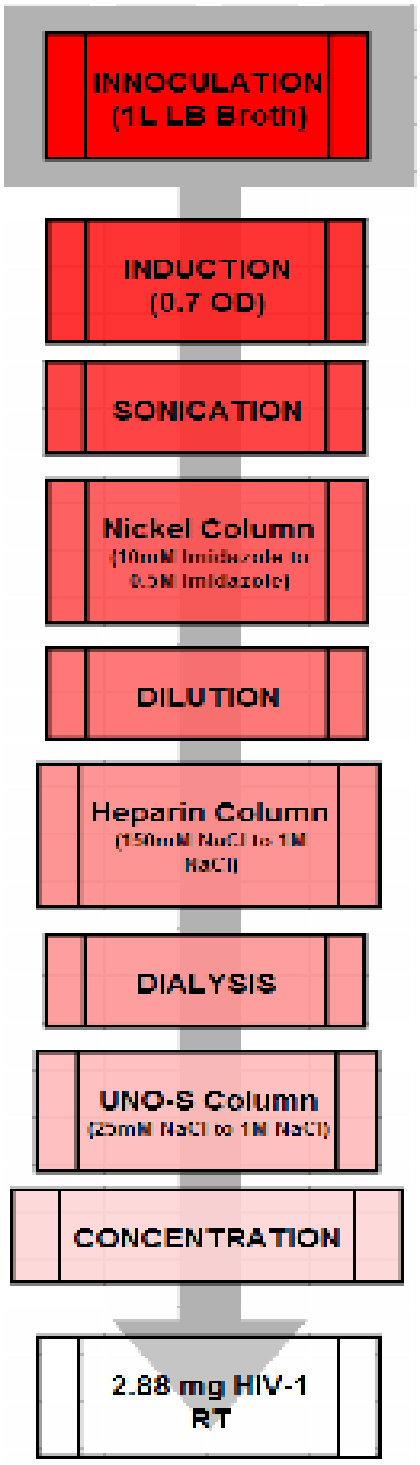

Figure 10. Purification scheme for HIV-RT, presenting the protocol adapted from Le Grice and associates [9].

Starting cell cultures of 1 to 4 liters were prepared in LB media with 100 ug/ml Ampicillin and 25 ug/ml Kanamycin at 37°C with shaking. Cultures were grown to 0.7 to 1.0 OD and then induced with 200 ug/ml IPTG. Following induction, the cultures were incubated for 5 hours and then pelleted by centrifugation.

Pellets, typically pinkish-colored, were frozen overnight in order to encourage lysis. The thawed pellets were then resuspended in 2 volumes (1ml/1g) of 50 mM sodium phosphate at pH 7.8 and with a final concentration of 1mM PMSF. Lysozyme was added to the resuspended cells to a concentration of 0.5 mg/ml and it was stirred slowly in the cold for 15-20 minutes. The cells were then lysed further by sonication and were centrifuged at high speed (25,000 rpm) for 2 hours.

Following centrifugation, the supernatant was decanted and dialyzed in 50 mM sodium phosphate buffer, pH 7.8 with 0.3M NaCl and 10 mM imidazole. The lysate was analyzed by SDS-PAGE and then passed through 3 successive purification columns (Figure 11).

For a 4-liter starting culture, 16 milliliters of Biorad Profinity^{Tm} Nickel-Charged affinity resin was packed in a 2

cm diameter column. The nickel column was equilibrated with 10 column volumes deionized water and 10 column volumes of 50 mM sodium phosphate buffer at pH 7.8 with 0.3M NaCl, 10 mM imidazole and 10% glycerol. The cell lysate was loaded onto the column at a flow rate of 0.5 ml/min and washed with 10 column volumes of 50 mM sodium phosphate with 0.3M NaCl, 10% glycerol, 10mM imidazole at pH6.0. HIV-RT was then eluted from the nickel column stepwise with increasing concentrations of imidazole from 10mM to 1M in 100 mM steps. The protein typically eluted at a concentration of 200mM imidazole in a single, homogenous peak.

Elution fractions collected from the nickel column were pooled, concentrated and analyzed by SDS-PAGE analysis. Since HIV-RT tends to adhere to Milipore^{Tm} filters, it was concentrated in a 12,000-14,000 MWCO dialysis bag covered in sucrose, allowing osmosis to remove excess water. The concentrated solution was then dialyzed in 50 mM sodium phosphate buffer, pH 7.0, with 25mM NaCl and 10% glycerol. After dialysis, the protein was loaded onto a 2 cm diameter column packed with 16 ml of Biorad heparin affinity resin and equilibrated with 10 column volumes of water and 10 column volumes of 50 mM sodium phosphate buffer, pH 7.0, with 150 mM NaCl and 10% glycerol. At a flow rate of 0.5 ml/min, the protein load was washed with the same equilibration buffer and eluted stepwise with an increasing concentration of NaCl from 150mM to 950 mM in 100 mM steps.

HIV-RT typically elutes from the heparin column at 300 to 350 mM NaCl and was collected in two or three fractions. The dilute protein solution was pooled, concentrated and analyzed by SDS-PAGE. After dialyzing overnight against 50 mM sodium phosphate, pH 7.0, with 25 mM NaCl and 10% glycerol, the sample was recovered and centrifuged at 20,000 rpm for 25 minutes to remove any precipitate. The clarified dialysate was loaded at 0.5 ml/min onto a 2 cm column, packed with 16 ml of Biorad UNO-Sphere^{Tm} ion-exchange resin. Prior to

loading, the column was equilibrated with 10 column volumes of water and 10 column volumes of 50 mM sodium phosphate buffer at pH 7.0, containing 25 mM NaCl and 10% glycerol. The protein load was then washed with 10 column volumes of the same buffer.

Stepwise buffer solutions from 25 mM NaCl to 1M NaCl were used to elute HIV-RT from the UNO-Sphere^{Tm} column. The protein typically eluted homogeneously at 225 mM NaCl. Elution fractions were pooled, concentrated and analyzed by SDS-PAGE. The final protein concentration was obtained using the Bradford assay [17]. Since a concentration of at least 0.2 mg/ml HIV-RT was necessary for analysis by CD spectroscopy, the protein was usually concentrated further at this point. While all of the HIV-RT produced during this study was immediately used for experimentation, it was kept in the refrigerator. For long-term storage, LeGrice and associates recommended dialyzing the purified HIV-RT against 50 mM Tris/HCl, pH 7.0, 25 mM NaCl, 1 mM EDTA, 50% (v/v) glycerol and storing at -25°C. Since Tris buffers tend to change pH with heating, a 50 mM sodium phosphate buffer should be used for storage.

B. CD Spectroscopy and Thermal Denaturation of HIV-RT

Prior to scanning, HIV-RT from the in-house purification was centrifuged at 20,000 rpm for 25 minutes in order to remove precipitate. The protein was analyzed by CD while in a 50 mM phosphate buffer, at pH 7.0, with 25 mM NaCl and 10% glycerol. HIV-RT was analyzed in a rectangular, 1 cm path length, screw-top cuvette. For one scan and thermal melt, the glycerol was dialyzed out of the buffer solution in order to evaluate its effect on HIV-RT stability. An AVIV Model 202 CD spectrometer was used to optically analyze the protein structure and unfolding. Spectra were initially observed at room temperature, at wavelengths of 200 nm to

245 nm in 1 nm steps in order to assess the secondary structure of HIV-RT and to ensure its proper folding. HIV-RT was then incubated at temperatures from 30°C to 90°C in 1°C intervals with 3 minute equilibration times in between each step.

Data was graphed, fitted and analyzed using the KaleidaGraph program (Synergy Software, Reading, PA, U.S.A.). The thermal denaturation curves generated by CD spectroscopy were fit to an adapted form of the van't Hoff equation, modified by Karantzeni and associates to directly evaluate thermal denaturation data [18]. The van't Hoff equation evaluates the transition between the native and denatured state of HIV-RT and upon fitting the melting curve, generates essential thermodynamic parameters.

$$\Delta\varepsilon = (m_n T + b_n) + (m_d + b_d)\left(\frac{K}{1+K}\right)$$

where $K = \exp[-\Delta H\,(1 - T / T_m)/RT]$

Equation 1. The van't Hoff Equation, modified by Karentzeni et al [18]. In this equation, the variables $m_{n,}$and m_d, represent the intercept and the slope of the native-state baseline of HIV-RT. The variables b_n and b_d represent the intercept and slope of the denatured-state baseline.

C. Thermal Stability Monitored via Nucleotide Incorporation by HIV-RT

For use in the nucleotide incorporation assay modified from Dowdy and associates by the LiCata laboratory, 27 unit/ul HIV-RT was purchased from Worthington ™ Biochemical Corporation [24]. According to the unit definition, one unit of HIV-RT incorporated 1 mole of titrated d-TMP into acid precipitable products using poly (A)/oligo (dt) 12-18 as the template/primer in 20 minutes at a pH of 8.3 and a temperature of 37°C. Efavirenz, acquired from the NIH AIDS Research and Reference Reagent Program, was diluted in 0.2% DMSO and added to the Worthington™ HIV-RT at a concentration of 1 uM. HIV-RT/efavirenz

solutions were preincubated prior to use in a nucleotide incorporation assay. Solutions of apo-HIV-RT were also prepared. The samples were heated to temperatures from 25°C to 75°C in 5°C intervals. Water baths were calibrated to this range of temperatures so that the samples could be heated individually prior to nucleotide incorporation. The preincubated HIV-RT with 1 uM efavirenz was added to a master mix to a final dilution of efavirenz of 0.0125 uM. The master mix contained a 10 mM Tris buffer with 25 mM KCl, 5 mM $MgCl_2$ and 0.1% Tween 20 at a pH of 7.9. In addition to buffer, the master mix contained 250 ug/ul sheared calf thymus DNA, 250 uM dNTP solution (with equal amounts of dCTP, dGTP and dTTP), and 187.5 uM dATP. In order to monitor HIV-RT activity during nucleotide incorporation, the master mix also contained 125 uCi/ml ^{32}P.

All preincubated samples were immediately cooled in a 25°C water bath for 1 minute prior to their addition to the master mix at the same temperature. Nucleotide incorporation by HIV-RT was limited to 30 minutes and the reaction was stopped by the addition of EDTA to the reaction solution. Aliquots of 10 ul were blotted onto 1.5 cm diameter trichloroacetic acid filters in order to precipitate long, assembled pieces of DNA. An extra filter for each preincubation temperature was prepared and analyzed without washing. The total count values from these unwashed filters were averaged in order to establish a total incorporation count for the assay. Additionally, master mix samples, exposed to EDTA but not to the HIV-RT were blotted and washed with the sample filters in order to establish a background. The remaining filters were washed in 3 successive, 5 minute washes with 50 ml of 300 mM sodium phosphate buffer at pH 7.0. Next, the filters were the washed for 1 minute in 70% ethanol with gentle swirling. After drying the filters were analyzed by a Packard TriCarb 2900™ liquid scintillation analyzer and the nucleotide incorporation values of efavirenz-bound HIV-RT and apo-HIV-RT were

compared to that of the background and unwashed samples. The nucleotide incorporation values were then plotted as a function of increasing preincubation temperature and the curves were fit to the van't Hoff equation.

III. Results

A. Purification of HIV-RT

Following a procedure developed by Le Grice and associates, HIV-RT was expressed and purified to homogeneity [9]. The recombinant, polyhistidine (His) tagged HIV-RT expression clone was obtained from the LeGrice laboratory and was expressed in *E. coli*. The protein was then sequentially purified by nickel, heparin and UNO-Sphere (ion-exchange) chromatography. Chromatographic elution profiles for each column are shown in Figure 11.

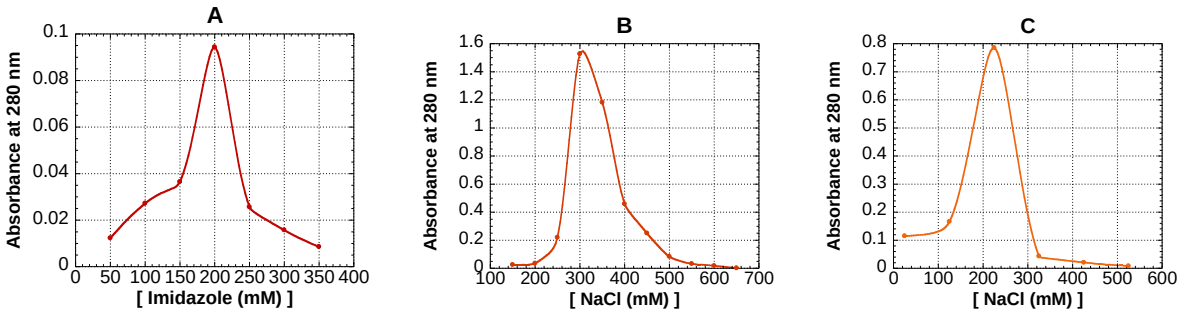

Figure 11. Stepwise elution profiles for the nickel column (A), heparin column (B), and UNO-Sphere column (C) used in HIV-RT purification. HIV-RT generally eluted in a single elution step from the nickel and UNO-Sphere columns; however, the protein eluted across 2 elution steps on the heparin column.

In addition to monitoring protein elution using spectrophotometry, the fractions collected during purification were also analyzed by sodium dodecyl sulfate polyacrylamide gel electrophoresis (SDS-PAGE). The gels, shown in Figure 12, present the gradual purification of HIV-RT with each successive column. When compared to the bands of the molecular weight standard, the two HIV-RT subunits appear consistently throughout the purification as bands at 51 kDa and 66 kDa. The gels from the heparin column frequently displayed bands that were not visible on the earlier nickel column gels. The appearance of these bands can most likely be

attributed to the increased concentration of HIV-RT in the nickel column elution as compared to the heparin column elution. The preparation typically yielded 2.0-3.0 mg of HIV-RT at 0.05 mg/ml prior to concentration from a starting culture volume of 3 liters. The LeGrice laboratory estimates HIV-RT purity at over 70% following this protocol although the HIV-RT that was produced in this study and theirs, as seen in Figure 12, shows a high degree of electrophoretically purity. It is not clear why LeGrice and associates estimates only a 70% purity for a sample resembling that in Lane 5 of Figure 12.

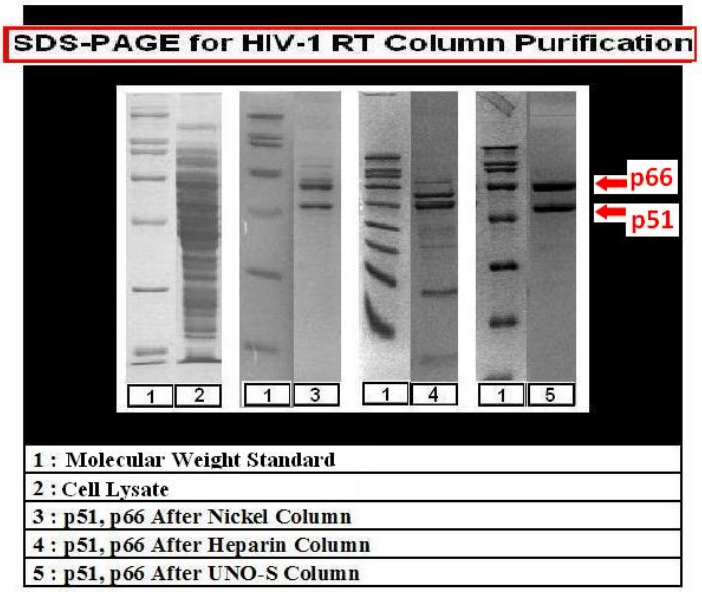

Figure 12. SDS-PAGE analysis of HIV-1 RT elution fractions, showing the purification of the p51 and p66 subunits using nickel, heparin and UNO-Sphere columns. Collected elution fractions are shown for each column. Lane 1 in each pair is the corresponding molecular weight standard from that gel.

While the LeGrice protocol was successfully replicated and scaled up in this study, not all of the protein preparations that were attempted yielded significant amounts of protein. For this study, a total of 6 preparations of HIV-RT were performed. Of those attempts, 4 yielded significant amounts of usable protein (between 1.5 and 3.0 mg/ml). Preparation #5 yielded inactive, insufficiently-purified HIV-RT, and preparation #6 did not produce a significant amount of protein. This gradual decrease in the production of usable amounts of active HIV-RT may likely have resulted from the continuous regeneration and reuse of affinity and ion exchange resins during the purification process.

B. Circular Dichroism (CD) Spectroscopy

Using the in-house purified HIV-1 reverse transcriptase, a series of biophysical studies were performed in order to better understand the properties of the protein. First, HIV-1 reverse transcriptase was concentrated and evaluated by circular dichroism (CD) spectroscopy. This technique detects structural asymmetry by measuring and comparing the absorption of left-handed and right-handed circularly polarized light. When no structural asymmetry is detected, the CD signal is zero; however, protein structures yield both positive and negative signals due to the stereo-chemical asymmetry of alpha helices and beta-sheets. This technique can be used to evaluate the ability of a particular protein to endure thermal and chemical stress, and it was first used in this study to confirm that the HIV-1 RT sample was folded (Figure 14).

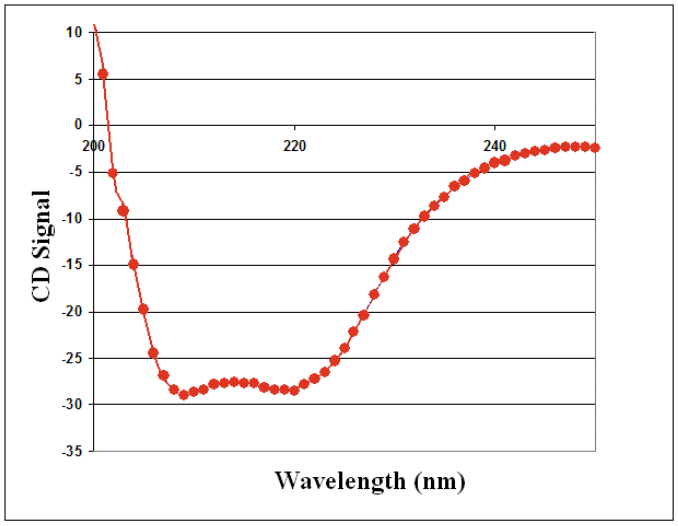

Figure 14. Room temperature (25°C) CD spectrum for HIV-1 RT, recorded at a concentration of 0.1 mg/ml, showing that the protein produced using the LeGrice protocol was folded following purification.

The HIV-RT CD spectrum was then compared to standard reference spectra in order to characterize the secondary structure of the protein (Figure 15).

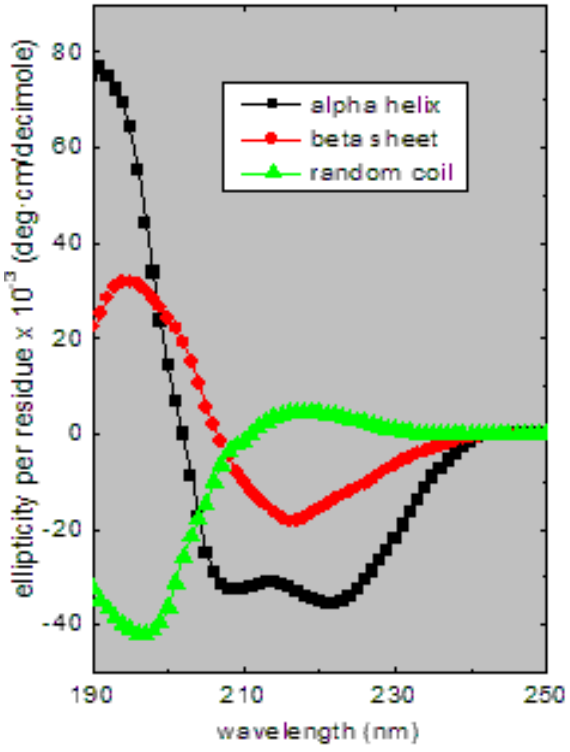

Figure 15. CD spectrum reference curves. The spectrum shown in black is characteristic of a predominately alpha-helical secondary structure while the red spectrum demonstrates the appearance of beta sheet secondary structure detected by CD spectroscopy. The random coil, shown in green, is characteristic of unfolded protein. This figure was taken from Alliance Protein Laboratories [26].

The CD spectrum of HIV-RT confirms that the secondary structure of the purified HIV-RT is predominately alpha-helical, as expected from the known crystal structure of the protein (Figure 2). Similar CD spectra are observed for other Type I DNA polymerases, such as Klentaq polymerase from *T. aquaticus* and Klenow polymerase from *E. coli* (Figure 16). The crystal structures of Klentaq and Klenow also confirm this structural similarity with HIV-RT (Figure 4).

C. Thermal Denaturation of HIV-RT

After observing the folded CD spectrum of HIV-RT at 25°C, the protein was thermally denatured and analyzed at 1°C intervals from 30°C to 90°C. The CD spectrum of HIV-RT was used to optically follow thermal denaturation. Four wavelengths near the spectral minimum were followed as increasing heat disrupted the predominately alpha-helical secondary structure of HIV-RT.

Tracking this transition as the protein unfolded produced a series of curves that could then be fitted to the van't Hoff equation and analyzed thermodynamically (Figure 17).

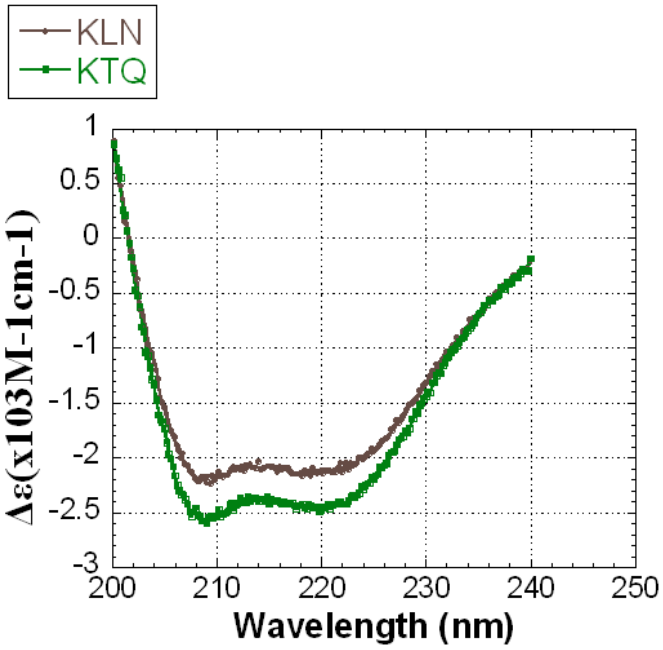

Figure 16. Room temperature (25°C) CD spectrum for Klenow (grey) and Klentaq (green) Pol I polymerases. This figure was adapted from Figure 6, Karantzeni et al. [18]

HIV-RT precipitated following thermal denaturation, indicating irreversible unfolding. Fully-reversible melting is required to obtain rigorous thermodynamic information from a thermal melt. Nevertheless, this is a preliminary study of HIV-RT and estimated thermodynamic parameters of HIV-RT unfolding were extracted from the CD data despite

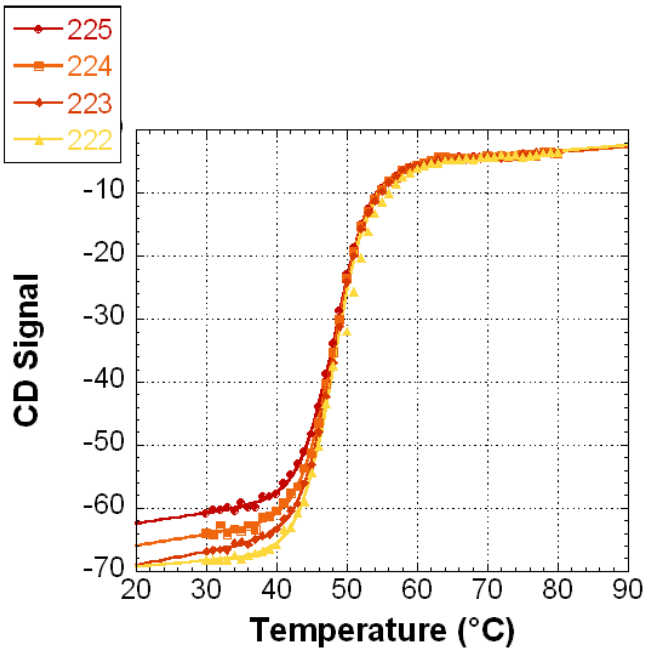

Figure 17. HIV-RT thermal denaturation from 30°C to 90°C monitored by CD spectroscopy. The protein was analyzed in a 50mM sodium phosphate buffer with 25mM NaCl and 10% glycerol at pH 7.0. The CD signal was monitored at wavelengths of 222 nm, 223 nm, 224 nm and 225 nm. The melting temperature (Tm) and apparent enthalpy of unfolding (ΔH^{app}) were determined from the van't Hoff equation used to fit the denaturation curves (Equation 1 in Methods).

precipitation. Irreversible thermal unfolding of larger proteins (>20 kDa) is very common. Thus, the van't Hoff enthalpy of HIV-RT unfolding (ΔH_{vH}) reported herein is an apparent value, or ΔH^{app}.

Data from four different wavelengths were fitted to a modified form of the van't Hoff equation. The fitted midpoint of the transition, which is the experimentally-determined Tm of HIV-RT is 48.3°C. The fitted ΔH^{app} was determined to be 84.2 kcal/mol. When compared to the thermal denaturation curves for Klenow and Klentaq polymerases, the HIV-RT unfolding curve appears more similar to that for Klenow, (Figure 18).

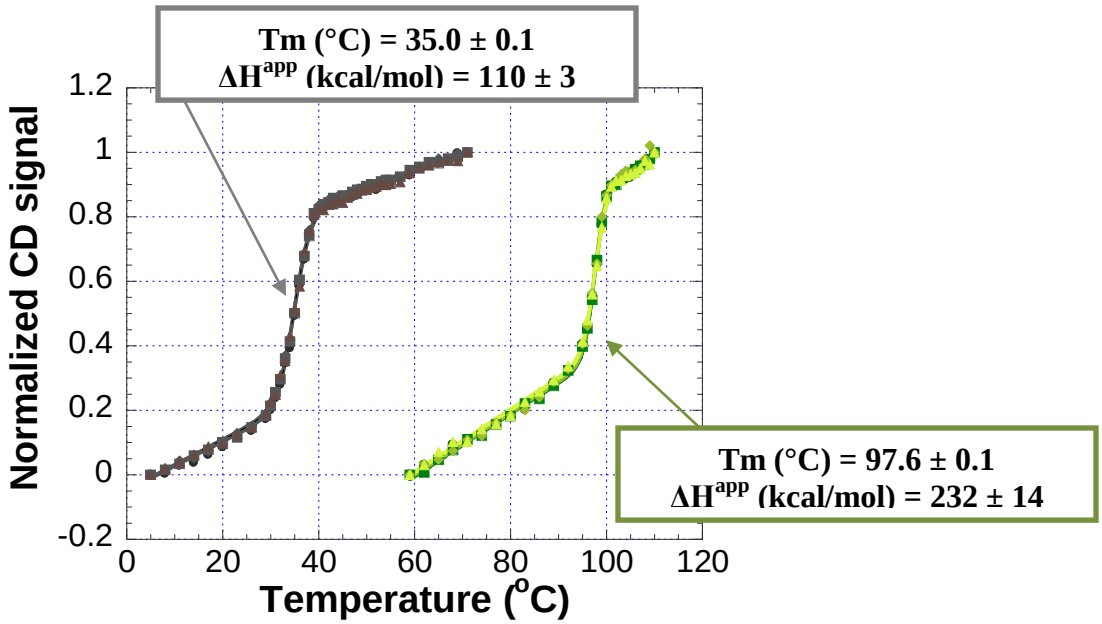

Figure 18. Normalized Klenow thermal denaturation (grey) from 5°C to 75°C monitored by CD spectroscopy, showing a two-state transition similar to that of HIV-RT. Also normalized, the Klentaq thermal denaturation from 59°C to 110°C monitored by CD spectroscopy, appears in green. These curves exhibits a two-state transition similar to that of HIV-RT. Klentaq melts at a much higher temperature because it is derived from the thermophilic bacterium *T. aquaticus*. Both plots show the signals at wavelengths of 222 nm, 221 nm, 220 nm and 219 nm. Both curves have been fitted to the van't Hoff equation. This figure was adapted from Figure 6, Karantzeni et al. [18].

When melted in a pH 7.0, 50mM sodium phosphate buffer with 25mM NaCl and 10% glycerol, HIV-RT exhibits a slightly higher Tm than the Klenow fragment as shown in Figure 18 where it was denatured in a pH 9.5, 10 mM potassium phosphate buffer, at 35.0°C. At pH and salt concentrations similar to that used for HIV-RT, however, Klenow has a Tm of approximately 52°C [19]. These pH 7.0 data for the Klenow fragment were obtained with a different type of assay, based on binding and fluorescence of 1, 8 anilinonaphthalene sulfonate (ANS), opposed to the CD signal versus temperature methods shown in Figures 17 and 18.

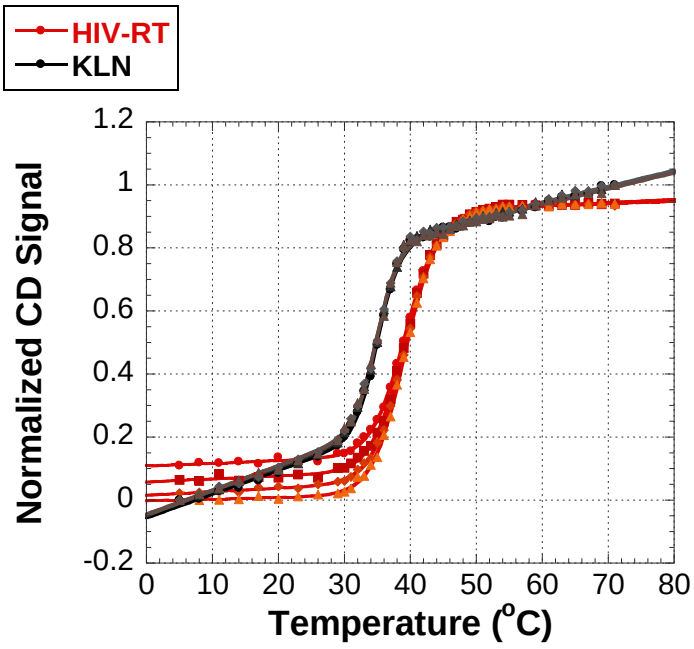

Figure 19. Normalized curves for HIV-RT and Klenow thermal denaturation, showing similar cooperativity and two-state transitions between the unfolded and native state.

The ΔH^{app} observed for Klenow at pH 9.5 is 110 kcal/mol, or 25.8 kcal/mol higher than the ΔH^{app} of HIV-RT. The ΔH^{app} was not determined at other pH values for Klenow. Cooperativity describes the sharpness of an unfolding transition, or how narrow or wide a temperature span is required for the transition region of the curve. When normalized and compared directly with Klenow, the thermal denaturation of HIV-RT exhibits a similar shape and cooperativity (Figure 19).

A more apparent shift in cooperativity is demonstrated when glycerol is removed from the buffer during the thermal denaturation of HIV-RT. When melted in the presence of glycerol, the protein exhibits a very cooperative, sharp, two-state curve. If glycerol is dialyzed out of the reaction buffer, HIV-RT generates a much more gradual, less cooperative melting curve (Figure 20). The removal of glycerol from the reaction buffer also causes a 1.8°C reduction in the Tm. Most published work on HIV-RT is done in the presence of 10% glycerol, due to its stabilizing properties.

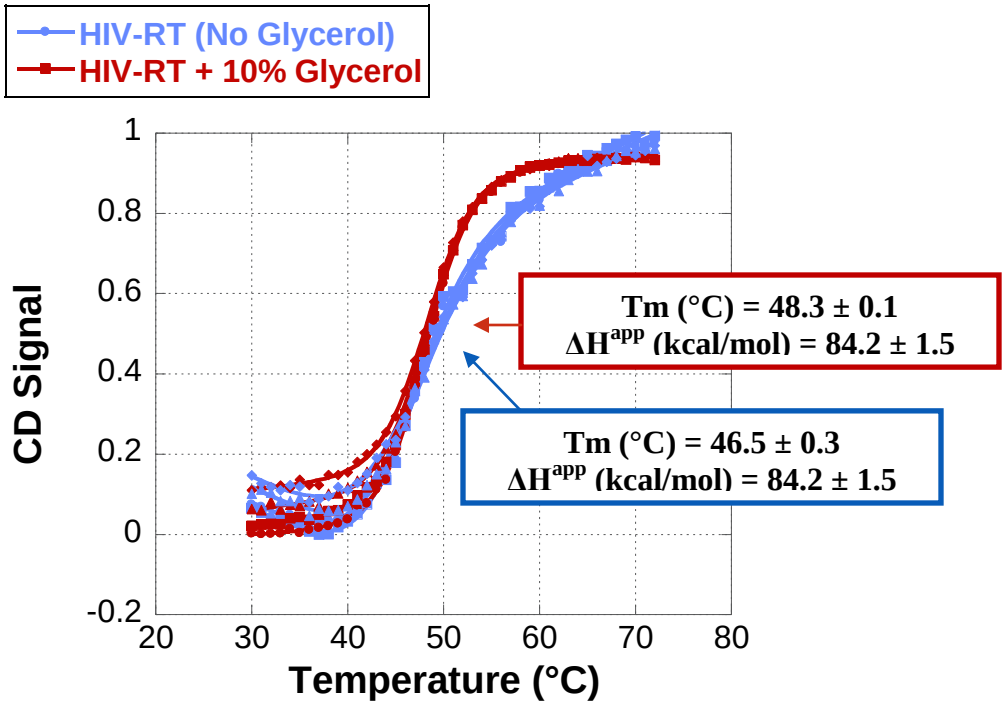

Figure 20. Normalized curves showing the effect of 10% glycerol on the thermal denaturation of HIV-RT in a pH 7.0, 50mM sodium phosphate buffer with 25mM NaCl.

Despite its dimeric structure, HIV-RT melts in a single step, or two-state transition between the native and unfolded state. This two-state transition implies the tight binding of the p51 and p66 subunits. Because of this tight binding, the subunits appear to dissociate and unfold in a single step, remaining noncovalently bound to each other until the point at which their

secondary structure denatures. This phenomenon has been observed in other oligomeric enzymes, such as aspartate transcarbamylase, or ATCase [21].

D. Thermal Stability Monitored via Nucleotide Incorporation by HIV-RT

A nucleotide incorporation based assay utilizing commercially acquired HIV-RT was designed and implemented in order to assess the effects of efavirenz on the stability of the enzyme. HIV-RT was incubated with and without efavirenz at temperatures from 25°C to 75°C and then used in a 25°C nucleotide incorporation assay. Depending on the extent of protein unfolding during the heat exposure, HIV-RT exhibited varying amounts of remaining activity. Thus, the nucleotide incorporation activity assay was used to monitor the thermal unfolding of HIV-RT and to investigate the effects of efavirenz on the structure of HIV-RT during the process of unfolding.

As efavirenz is an NNRTI, it significantly reduces the nucleotide incorporation rate of HIV-RT. In fact, the drug works so effectively in vitro that it had to be diluted to a concentration of 1uM and included only in the preincubation step of the assay. When used at higher concentrations such as the 25 uM concentration used in Barkley and associate's studies of HIV-RT dimerization, nucleotide incorporating activity was completely inhibited. In order to monitor the effects of the drug on HIV-RT nucleotide incorporation, exposure to 1 mM efavirenz had to be limited to the preincubation, temperature exposure step, and then diluted to 0.0125 uM during the actual incorporation reaction, allowing the protein to be active during the assay.

As an alternative to the 1 uM dilution method used to evaluate the effect of Efavirenz on HIV-RT during the preincubation step, Sephadex spin columns were also tested as a method of removing the drug after thermal incubation but before the incorporation assay. While this

method did remove enough Efavirenz to allow HIV-RT to exhibit nucleotide incorporation activity, it yielded lower activity than the dilution method. This reduction in nucleotide incorporation may likely have been due to protein loss during spin column filtration. In future repetitions of this procedure, optimizing the use of spin columns may reduce protein loss while effectively removing Efavirenz from the preincubation solution prior to nucleotide incorporation.

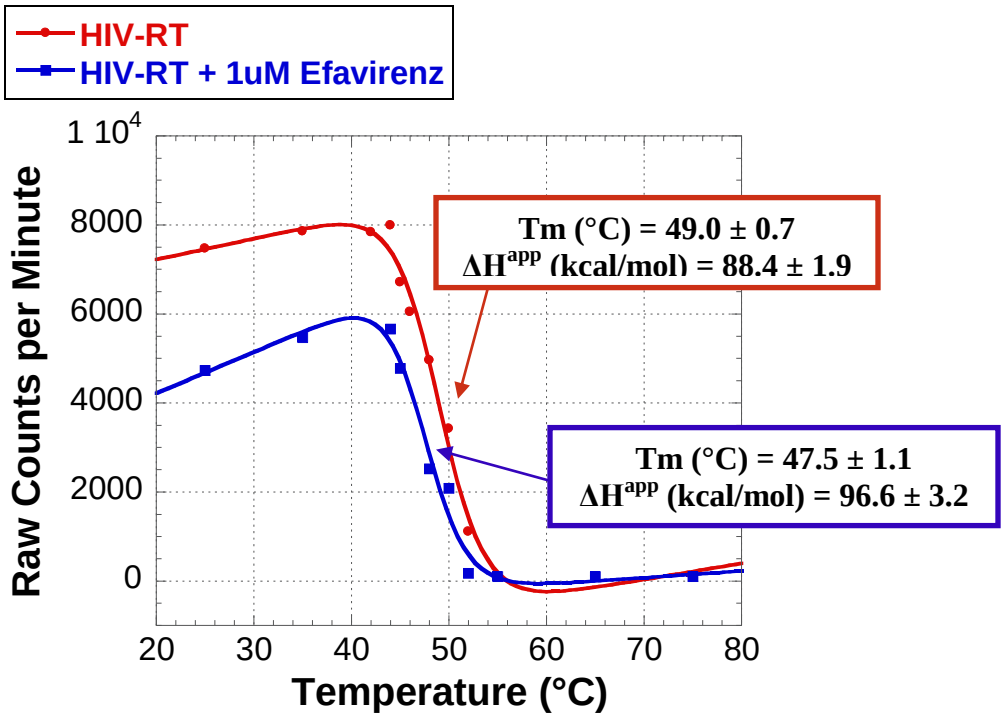

Figure 21. The effect of increasing preincubation temperature on HIV-RT nucleotide incorporation with and without Efavirenz. Both curves have been fitted to the van't Hoff equation. The Tm and curve for HIV-RT, incubated alone at increasing temperature, is shown in red. When incubated with Efavirenz at increasing temperature, HIV-RT exhibited a lower Tm and nucleotide incorporation activity (shown in blue).

Based on the sedimentation equilibrium studies of Barkley and associates, Efavirenz was predicted to allosterically increase the binding affinity between the p51 and p66 subunits of HIV-RT [8]. It was thus hypothesized that when melted, HIV-RT would exhibit an increased Tm

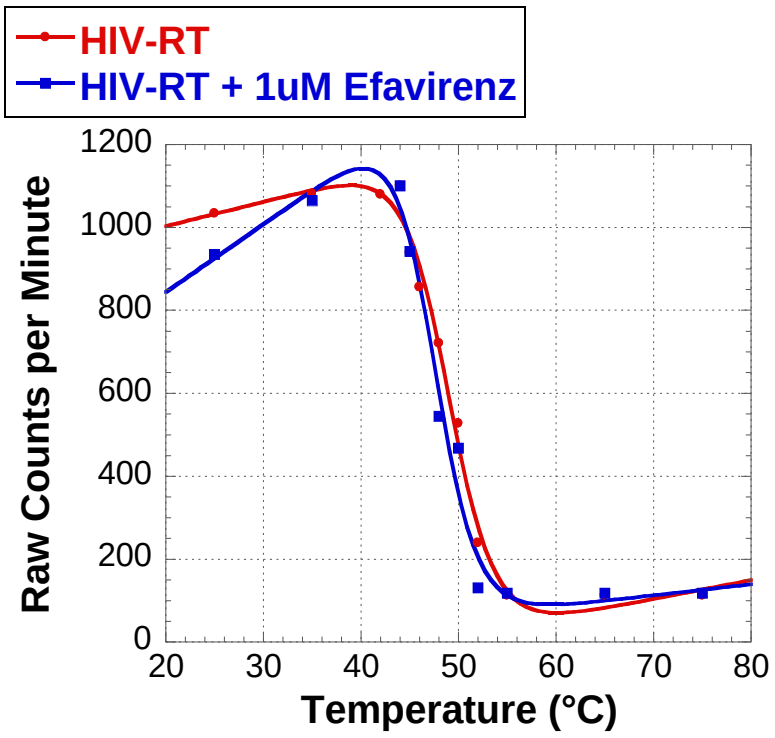

Figure 22. Normalized graph showing the effect of Efavirenz on HIV-RT nucleotide incorporation. Both curves have been fitted to the van't Hoff equation.

when bound to Efavirenz. However, HIV-RT exhibited a Tm that was 1.5°C lower when incubated with Efavirenz prior to nucleotide incorporation but even this slight shift is within the statistical error of the two denaturations (Figure 21).

If anything, efavirenz appears to have had a slightly destabilizing effect on HIV-RT, causing the activity of the protein to decrease at a lower temperature although statistically, the two Tm's are equivalent. The constant Tm contrasts with the stabilizing effect and increased Tm that was predicted based on Barkley and associates' Analytical Ultracentrifugation (AU) data [8]. The difference in nucleotide incorporation at lower temperatures for HIV with and without efavirenz (i.e. where each curve in Figure 21 intercepts the y-axis) can most likely be attributed to the use of the dilution method for drug preincubation.

Although efavirenz was at 1 uM during heating with HIV-RT and then further diluted during nucleotide incorporation, the drug was not eliminated from the assay. A small amount of

efavirenz was carried into the nucleotide incorporation assay and additionally influenced the activity of HIV-RT. Full elimination of the drug from the nucleotide incorporation would be the best scenario for more clearly understanding the interaction between HIV-RT and Efavirenz.

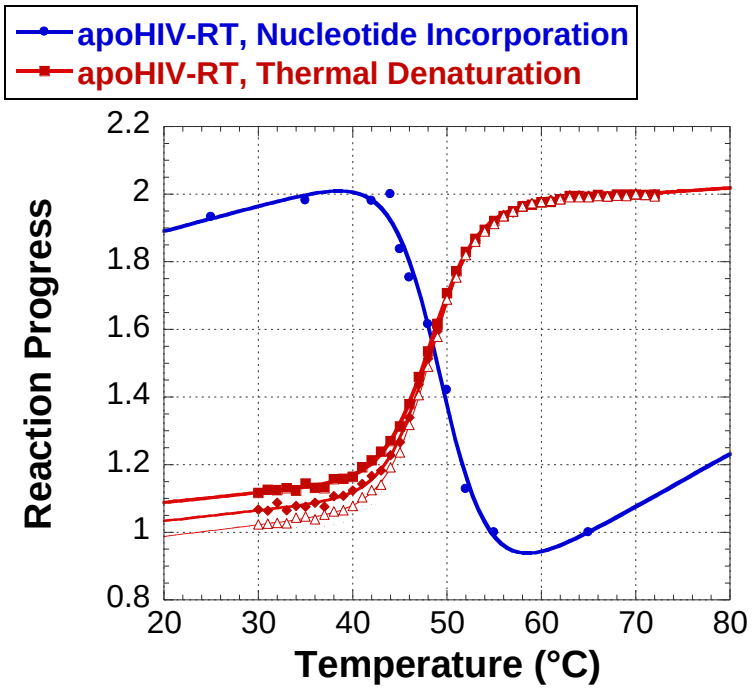

Figure 23. Normalized curve from nucleotide incorporation without Efavirenz plotted with the curve generated during HIV-RT thermal denaturation by CD spectroscopy. The two melting curves exhibit a similar Tm of 48°C.

The nucleotide incorporation curves for HIV-RT with and without Efavirenz were normalized and plotted together to give a clearer illustration of the minimal effect efavirenz has on the unfolding of the protein (Figure 23). Interestingly, Efavirenz does not appear to alter the shape or cooperativity of the curve.

When normalized and plotted together, the nucleotide incorporation data for the unbound protein and the CD melting curves clearly overlap at a Tm of 48°C (Figure 23).

The fact that the nucleotide incorporation assay and the thermal denaturation of HIV-RT by CD spectroscopy yielded similar Tm values demonstrates that monitoring HIV-RT activity tracks with protein unfolding and subunit dissociation. It also reinforces the validity of using the nucleotide incorporation assay to evaluate the effect of efavirenz on HIV-RT stability.

V. Discussion

A. Purification of HIV-RT

As this was the first purification of HIV-RT in the LiCata laboratory, there is certainly room for technical improvement in order to increase the efficiency and yield of the protocol adapted from LeGrice. Possible improvements to the protocol may also help avoid the problems that occurred in the two failed protein preparations. Although the LeGrice laboratory typically uses a continuous gradient to elute HIV-RT from each column, stepwise elution was used for 5 of the 6 purifications. This method was more easily applied in the purifications with 1 and 2 liter starting cultures. When the starting culture volume was scaled up to 3 liters, stepwise elution became considerably more time-consuming and labor-intensive. A gradient elution method was used in HIV-RT preparation 5; however, a failure to control the column flow rates may have resulted in substandard purification. Although additional attempts to use gradient elution will require some troubleshooting, they may ultimately improve the protocol developed in this study (Appendix A).

Another area of improvement of the HIV-RT purification protocol used in this study may lie in column packing and column equilibration, with the use of a peristaltic pump to maintain a constant flow rate of 0.5 ml/min. This technique was implemented during the final protein preparation. While attempt #6 did not result in a substantial yield of HIV-RT, the elution time for the purification was greatly improved and the flow rate was more easily controlled. A combination of older, exhausted resins and excessive column back pressure may account for the failure of this final purification. Optimizing use of the pump to pack, equilibrate, load and run

columns in future protein preparations can likely improve the current protocol and increase the yield and purity of HIV-RT.

For future studies, in addition to optimizing and expediting the native heterodimeric HIV-RT purification protocol, it would be useful to purify the p51 and p66 subunits individually. The selective expression of p66 could be made possible by using an RT coding sequence without HIV-PR. In the absence of this modifying enzyme, the p66 subunit would not be cleaved and the cell lysate would contain only homogenous p66 HIV-RT (Figure 24).

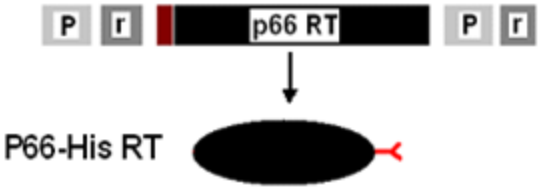

Figure 24. (A) Expression of HIV-RT subunit p66 using an expression cassette lacking a coding region for HIV-PR. Without HIV-PR, the larger subunit is not cleaved between the Tyr-441 and Phe-440 residues and p51 is not generated. (B) After induction, lysis and analysis by SDS-PAGE, the LeGrice laboratory was able to produce homogenous p66 which could then be purified using the protocol for p51/p66 HIV-RT. This figure adapted from Figure 1 by LeGrice and associates [9].

Two additional plasmids, p6H RT for p66 and p6H RT51 would be necessary for the expression of the individual subunits. Purifying the subunits individually will most likely be essential to future studies on HIV-RT stability and dimerization. (Potential experiments on homogenous p66 and p51 are discussed later.) Therefore, there is additional room for improvement, modification and specialization of the protocol adapted from the LeGrice laboratory.

B. CD Spectroscopy and Secondary Structure of HIV-RT

Given the relatively large amount of HIV-RT that is required for analysis by CD spectroscopy and other biophysical methods, it is essential for this laboratory to optimize the LeGrice-adapted purification protocol. While good CD spectra and thermal denaturation curves were obtained from the in-house purified HIV-RT, they were obtained through a great deal of trial and error. HIV-RT was most successfully analyzed by CD spectroscopy at a concentration of 0.2 mg/ml in a 1 cm path length, 3.5 ml cuvette. This amounted to roughly 25% of the HIV-RT produced from a single preparation. Increased protein yield would definitely be necessary for future CD analysis of HIV-RT.

The CD spectrum generated by HIV-RT is very similar to that of Klenow and Klentaq polymerases (Figures 15 and 16). Predominantly alpha-helical, the three proteins also demonstrate similarities in quaternary structure (Figure 5). The right hand-shaped domain structures of Klenow and Klentaq are comparable to HIV-RT, with clearly-defined "palm", "thumb" and "finger" regions. This consistency in structure confers common function among the three enzymes. The palm domain is attributed with catalyzing the phosphoryl transfer reaction of DNA polymerization and it remains homologous in RT, pol I and pol I polymerases [22].

The CD spectrum obtained for HIV-RT in this study will be useful in further analysis of heterodimeric, homodimeric and monomeric HIV-RT. The spectrum can be used in combination with the protein purification in order to assess the degree of proper folding and, consequently, the quality, of the in-house HIV-RT. Additionally, it would be interesting to compare CD spectra from individually-purified p51 and p66 subunits. As p51 lacks an RNase H domain as a

result of its post-translational modification from p66 by HIV-PR, it would most likely exhibit a slightly different CD spectrum. Further analysis by CD Spectroscopy would be beneficial to an increased understanding of the dimerization interaction of the p51 and p66 subunits.

C. Thermal Denaturation of HIV-RT

When compared to melting curves for Klentaq and Klenow, the melting curve for HIV-RT appears very similar – it appears two-state and has similar cooperativity. However, the thermal denaturation behavior of HIV-RT is much more similar to that of Klenow. This was not entirely expected. While HIV-RT is by no means thermophilic, it is dimeric and possesses internal, noncovalent bonding between the p51 and p66 subunits. Protein dimerization causes an increase in the free energy (ΔG) of stabilization. The p51 and p66 monomers actually bind to one another, with a favorable free energy of binding. Therefore, the dimerization of the p51 and p66 subunits must contribute considerably to the overall stability of HIV-RT.

Thus, the stability of HIV-RT was hypothesized to be much higher than that of Klenow. As noted in the results when melting data for Klenow are obtained in solution conditions most similar to those used here for HIV-RT, Klenow actually even has a higher Tm than HIV-RT. The thermal denaturation of the p51 and p66 subunits would most likely yield lower Tm values than the 48.3°C Tm of heterodimeric HIV-RT. The difference in Tm's from the heterodimeric and monomeric melts could be compared in order to ascertain the amount of stability gained by the dimerization of the subunits.

In addition to separately melting the p51 and p66, it would be useful to use CD spectroscopy to monitor the chemical denaturation of HIV-RT with guanidine or urea. HIV-RT

generated a thermal denaturation curve that was successfully fit by the van't Hoff equation; however, the protein precipitated with heating over 90°C, rendering the reaction irreversible. While Klenow and Klentaq both precipitate with melting, they are reversibly denatured by chemical means. If HIV-RT could be reversibly denatured with either guanidine or urea, the thermodynamic parameters generated from the CD data for HIV-RT would be validated. Chemical denaturation would also provide information on the ΔG of folding that thermal denaturations do not.

D. Thermal Stability Monitored via Nucleotide Incorporation by HIV-RT

The precise molecular effect that NNRTIs have on HIV-RT is widely debated among researchers. While the drugs function in slowing the rate of nucleotide incorporation by the enzyme, the exact mechanism that causes this reduction in activity is not well understood. Multiple mechanisms have been proposed in order to describe the complex reaction that NNRTIs have on HIV-RT, attributing NNRTI effectiveness to an allosterically modification of the active site as well as to the p51/p66 interface. In comparison to the surface between the two subunits, the NNRTI binding pocket is very small (Figure 25). It is not yet understood if the subunit association effects of NNRTI's are localized to near the binding site, or de-localized to alter the entire surface of the binding interface of p51 and p66.

Due to the complexity of this allosterically-mediated alteration of the subunit interface of HIV-RT, Tachedjian and associates postulate that the NNRTIs must act by other mechanisms in addition to enhancing the noncovalent linkages between p51 and p66 [14]. Using a yeast two-hybrid assay, they observed that efavirenz binds more tightly to p66 than to p51 and also

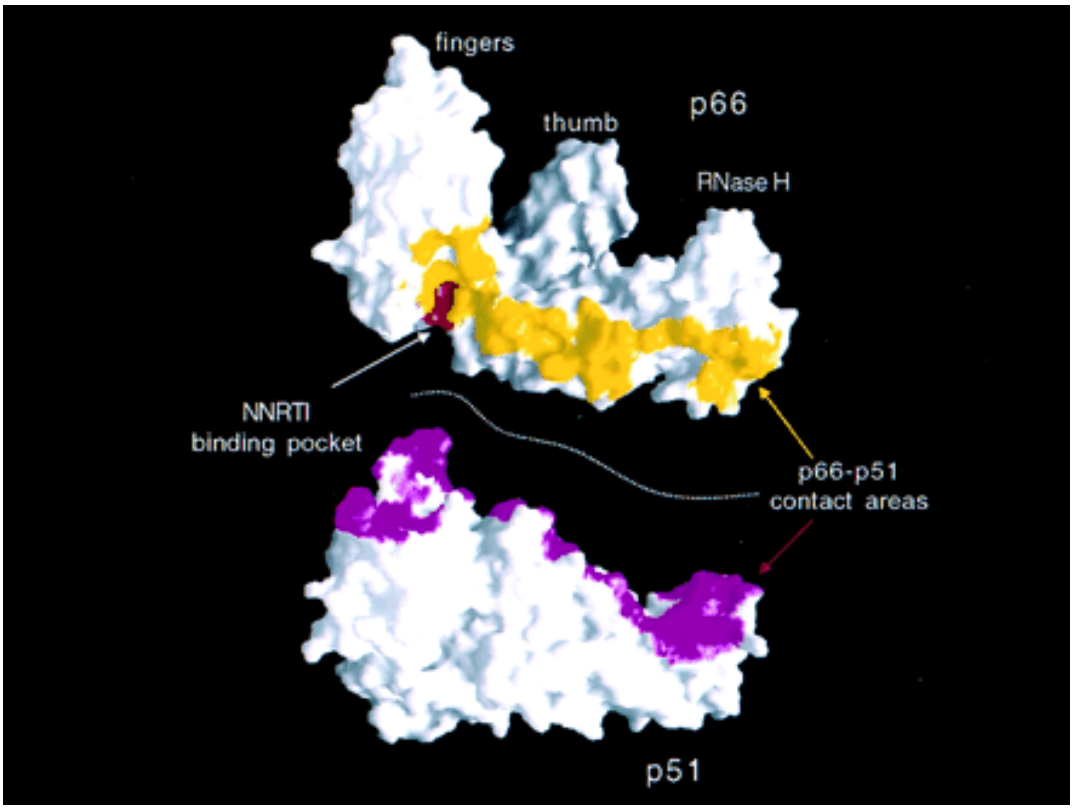

Figure 25. Surface representation of the p51 and p66 HIV-RT subunits, comparing the size and location of the NNRTI binding pocket on the p66 subunit to that of the interface between the two monomers. The NNRTI binding pocket (shown in red) is shown in relation to the regions of HIV-RT that are not exposed solvent when the enzyme is in solution in its heterodimeric form (shown in gold on p66 and in purple on p51). This figure is from Tachedjian and associates, Figure 1 [X].

established that the drug increases dimerization and, as a result, the stability of the p51/p66 interface [14]. Mary Barkley and associates came to a similar conclusion using analytical ultracentrifugation of efavirenz-bound HIV-RT [15].

In this thermodynamic study of efavirenz-bound HIV-RT, the protein-ligand complex did not exhibit a Tm that was significantly higher than the apo-protein (Figure 23). When efavirenz (or any ligand) binds to HIV-RT (or any protein), the free energy of its binding is added to the original stabilization energy of the apo-protein. When HIV-RT is unfolded, the total free energy of the efavirenz-bound enzyme must increase. According to Barkley, efavirenz considerably

increases subunit dimerization from that of the apo-protein. While this effect, combined with the simple ligand-protein interaction must increase the free energy of stabilization, this increase was not reflected by the Tm of efavirenz-bound HIV-RT when compared to the apo-protein.

Although shifts in Tm are commonly used to detect changes in ΔG, the variables cannot always be translated. The two values are related non-linearly although one usually confers the other, exceptions do exist [19]. In this case, neither the drug binding nor the enhanced dimerization effect was reflected in a shift in Tm. While it is difficult to interpret these results, there are potential explanations for this "disappearance" of free energy. When the nucleotide incorporation curves of efavirenz-bound HIV-RT and apo-HIV-RT were fit to the van't Hoff equation, the drug-bound protein exhibited a ΔH^{app} that was 8.2 kcal/mol more favorable than that of the protein in its native state. This enthalpic difference accounts for the expected increase in the ΔG.

Another useful application of CD spectroscopy to the study of HIV-RT stability and dimerization would involve the thermal denaturation of the protein in the presence of efavirenz. This would allow for a direct analysis of the effect of the drug on the stability of the protein and on the tightness of the noncovalent binding of the p51 and p66 subunits. The Tm generated from the van't Hoff fit of the apo-HIV-RT melting curve could then be directly compared to the Tm resulting from the efavirenz-bound HIV-RT in order to ascertain the effect of the drug on protein stability and subunit interaction. This technique should also be used to analyze the effect of other NNRTIs such as nevirapine and etravirine on the stability of HIV-RT and the interaction of p51 and p66 as no one has yet looked at these NNRTI's relative to subunit association and protein stability.

While thermal stability was monitored via nucleotide incorporation by HIV-RT, this is an indirect method for ascertaining the effect of efavirenz on subunit dimerization. Thermally denaturing HIV-RT and observing its activity did generate a curve that fit the van't Hoff equation and produced a Tm consistent with the CD melt data. Nevertheless, tracking HIV-RT unfolding as a function of its activity is an indirect reflection of denaturation as compared to CD spectroscopy. While thermal melts by CD require larger quantities of HIV-RT, this technique would allow for a direct observation of the effect of efavirenz, and any other NNRTI, on HIV-RT stability and dimerization.

Since effective protein-ligand interactions typically result in observable shifts in the melting temperatures of target enzymes, major pharmaceutical companies frequently Tm values to screen drugs. This technique operates on the assumption that an increase in the Tm of a bound target protein, in comparison to its native state, indicates tighter ligand binding and increased free energy change. Compounds that do not significantly alter the Tm of the native state are discarded and not investigated further. When considering the results generated in this study, Tm may not always be an effective criterion for judging the effectiveness of compounds during drug screening. Efavirenz-bound HIV-RT demonstrated a Tm that was consistent with than that of apo-HIV-RT. Despite the drug's effectiveness at slowing nucleotide incorporation in vitro and its dramatic effect on HIV-RT dimerization, it would have likely been overlooked during screening.

The example of efavirenz-bound HIV-RT attests to the importance of using multiple criteria in drug screening. It also presents the necessity for a more thorough understanding of the interaction between commonly-prescribed, commercially-produced drugs and their target proteins. A better understanding of the dimerization effect of NNRTIs such as efavirenz on

HIV-RT could be usefully applied to antiretroviral drug development in two ways. Elucidating the precise mechanism by which these drugs allosterically modify HIV-RT and render it inactive would provide researchers with the information necessary to improve the NNRTIs in new and effective ways. Second, p51/p66 dimerization has been targeted by groups such as Tachedjian and associates as a route to peptide drug development. Small compounds that block the subunit dimerization of HIV-RT are currently being investigated as an alternative to NNRTIs. While anti-dimerization HIV-RT peptide drug development is in its early stages, the new compounds could provide a way to effectively combat NNRTI-resistant HIV.

VI. References

1. V. Vivet-Boudou, J. Didierjean, C. Isel, R. Marquet, *Cell. Mol. Life Sci.* 2006, *63*, 163-186.

2. Tantillo et al., *J. Mol Bio*. 1994, *243*, 369-397.

3. A. M. Barber, A. Hizi, J. R. Maizel, S. H. Hughes, *AIDS Res. Hum. Retroviruses* 1990, *6*, 1061-1072.

4. J.M. Navarro, L. Damier, J. Boretto, et al. *Proc Natl Aca Sci USA* 1993, *90*, 6320-6324.

5. A Jacobo-Molina, J Ding, R G Nanni, A D Clark, Jr, X Lu, C Tantillo, R L Williams, G Kamer, A L Ferris, P Clark, *Science*, 1992, *256*, 1783-1790.

6. Zhang H-J, Wang Y-X, Wu H, Jin D-Y, Wen Y-M, et al, *Proc Natl Acad Sci U S A*, 1993, *90*(13), 6320–6324.

7. Kalyan Das, J.D. Bauman, A. D. Clark Jr., Y. V. Frenkel, P. J. Lewis, A. J. Shatkin, S. H. Hughes, E. Arnold, *Proc. Natl. Acad. Sci. USA*, 2008, *105*, 1466-1471.

8. M. E. Ignatov, A. J. Berdis, S. F. J. Le Grice, M. D. Barkley, *Biochemistry* 2005, *44*, 5346-5356.

9. S. F. J. Le Grice, G. E. Cameron, S. J. Benkovic, *Methods in Enzymology*, 1995, *262*, 130-144.

10. SJ Smerdon, J Jager, J. Wang, LA Kohlstaedt, AJ Chirino, JM Friedman, PA Rice, and TA Steitz, *Proc. Natl. Acad. Sci. USA*, 1994, *91*, 3911-3915.

11. JC Wu, TC Warren, J Adams, J Proudfoot, J Skiles, P Raghavan, C Perry, I Ptotcki, PR Farina, and PM Grob, *Biochemistry*, 1991, *30*, 2022-2026.

12. M J Zapor, KL Cozza, GH Wynn, GW Wortmann, SC Armstrong, *Psychosomatics*, 2004, *45*(6), 524-535.

13. A Figueiredo, KL Moore, J Mak, N Sluis-Cremer, M de Bethune, and G Tachedjian, *PLOS*

Pathogens, 2006, *2*(11), 1051-1059.

14. G Tachedjian and SP Goff, *Curr Opin Investig Drugs*, 2003, *8*, 966-73.

15. Carl F. Venezia, Kathryn J. Howard, Michael E. Ignatov, Leslie A. Holladay, and Mary D. Barkley, *Biochemistry*, **2006**, *45* (9), 2779–2789.

16. DrugBank Website (http://www.drugbank.ca/drugs/DB00625).

17. MM Bradford, *Anal. Biochem.*, 1976, *72*, 248-254.

18. I Karantzeni, C Ruiz, C Liu and VJ Licata, *Biochem J.*, 2003, *374*, 785-792.

19. AJ Richard, C Liu, AL Klinger, MJ Todd, TM Mezzasalma, VJ LiCata, *Biochimica et Biophysica Acta 1764*, 2006, 1546-1552.

20. D Deredge, G Thompson, K Jiang, S Patel, K Datta, and V LiCata, *Biophysical Journal*, 2009, *96*, 418a-419a.

21. VJ LiCata, and NM Allewell, *Biophysical Chem*., 1997, *62*, 225-234.

22. TA Steitz, *The Journal of Biological Chemistry*, 1999, *274*, 17395-17398.

23. Ren J, Bird LE, Chamberlain PP, et a.l, *Proc Natl Acad Sci USA*, 2002, *99*, 14410–15.

24. K Li, W Lin and K Chung, BM Moore, and M. B. Doughty, 2002**,** *Bioorganic and Medicinal Chemistry* , *10*, 507-515.

25. Alliance Protein Laboratories Website (www.ap-lab.com/circular_dichroism.htm).

VII. Appendix

A. Modified LeGrice Protocol for HIV-RT Purification

HIV-1 RT Purification 08/19/2008

BUFFERS

1. 50 mM NaP pH 7.8 $NaPO_4$
2. 50 mM NaP pH 7.8, 0.3 M NaCl, 10% Glycerol, 10 mM imidazole
3. 50 mM NaP pH 6.0, 0.3 M NaCl, 10% Glycerol, 10 mM imidazole
4. 50 mM NaP pH 7.0, 25 mM NaCl, 10% Glycerol
5. 50 mM NaP pH 7.8, 150 mM NaCl, 10% Glycerol
6. 50 mM NaP pH 7.0, 1 M NaCl, 10% Glycerol
7. 50 mM NaP pH 7.0, 25 mM NaCl, 1 mM EDTA, 50% Glycerol

DAY 1

Plates
2.5 g LB media
1.5 g agar
100 ml H_2O
Autoclave
100 ug/ml Ampicillin (1ml H_2O/100 mg Amp., need 5 ul)
25 ug/ml Kanomycin (1ml H_2O/25 mg Kan., need 2 ul)
Temper agar until it is cool to touch
Pour plates and allow to solidify
Once solidified, turn plates cover side down to dry overnight
Streak plates with stored culture (-80°C)
Incubate plates at 30°C 12-16 hrs

DAY 2

5 ml LB Starter Culture
Make 50 ml of above media (DAY 1)
Add 5 ml LB to sterile tube (1 for each 1L starter culture)
Inoculate LB with a single LeGrice colony per tube
5 ul of 100 ug/ml Ampicillin
2.5 ul of 25 ug/ml Kanomycin
Let grow at 37°C for 8 hours with shaking (cover with cap loose to let breathe)

DAY 3

1L Starter Culture
25 g LB media
Bring up to 1L volume
Autoclave
1000 ul 100 ug/ml Ampicillin filter into liter
500 up 25 ug/ml Kanamycin filter into liter

DAY 3 (contd.)

Inoculate with 5 ml LeGrice starter culture
Take initial OD reading
Allow to grow at 37°C with shaking
Take OD reading every 30 mins until culture reaches an OD of 0.7-1.0

Induction

Induce with 200 mg/ml IPTG
Let grow at 37°C for 5 hours after induction

Harvesting

Record mass of empty 500 ml bottles
Harvest in two 500 ml bottles by centrifuging at 6500 for 20 mins at 4°C
Pour off supernatant media in one continuous pour (pellet is pinkish)
Record mass of bottles with pellets and subtract initial mass to get cell weight
Freeze pellets overnight

DAY4

Prepare PMSF
- Add up cell weights and multiply by 2 vol
- Dissolve in 10 ml isopropyl alcohol
- Heat slowly in hot water bath, periodically opening cap to release pressure
- Close and vortex until all crystals are dissolved

Multiply cell weight by 4 and add that amount of buffer #1
Add PMSF to the buffer to a concentration of 0.2 M
Add 10 ml buffer #1 to each of the bottles
Resuspend cells in buffer with PMSF using a policeman
Use a 10 ml pipette to measure volume of suspended cells, add to beaker
Add 5 ml buffer to bottles and collect remaining cells with a transfer pipette
Add lysozyme to 0.5 mg/ml, stir in cold for 20 mins on low

Sonication

Sonicate on duty cycle 40, output control 5, 5 to 6 times with 1sec on/1 sec off
Repeat for 1 min with 1 min rest time in between (keep on ice)
Transfer lysate to small centrifuge tubes
Centrifuge at 20,000 rpm for 1.5 hours (25.5 rotor)
Decant supernatant into graduated cylinder
Dialyze overnight in buffer #2

DAY 5

Nickel Column Purification

Load and run SDS-PAGE of lysate
Take OD reading

Pack 1.5 cm diameter column with 16 ml of nickel affinity resin
Equilibrate with 10 CV water and 10 CV buffer #2

DAY 6 (contd.)

Centrifuge HIV-RT lysate at 20,000 rpm for 20 mins to remove precipitate

Load HIV-RT lysate at 0.5 ml/min

Wash with 10 CV buffer #2 and 10 CV buffer #3

Elute with a 10 CV gradient (stepwise) of 50 mM NaP pH 6.0, 0.3 M NaCl, 10% Glycerol, 10 mM imidazole →50 mM NaP pH 6.0, 0.3 M NaCl, 10% Glycerol, 1 M imidazole

Concentrate in dialysis bag, cover in sucrose, watch to prevent precipitation

Collect fractions and analyze with SDS-PAGE

Dialyze overnight against buffer #4

DAY 7

Heparin Column

Centrifuge HIV-RT lysate at 20,000 rpm for 20 mins to remove precipitate

Load HIV-RT lysate at 0.5 ml/min

Wash with 10 CV buffer #5

Elute with a 10 CV gradient (stepwise) of 50 mM NaP pH 7.8, 150 mM NaCl, 10% Glycerol → 50 mM NaP pH 7.8, 1M NaCl, 10% Glycerol

Concentrate in dialysis bag, cover in sucrose, watch to prevent precipitation

Collect fractions and analyze with SDS-PAGE

Dialyze overnight against buffer #6

DAY 8

UNO-Sphere Column

Centrifuge HIV-RT lysate at 20,000 rpm for 20 mins to remove precipitate

Load HIV-RT lysate at 0.5 ml/min

Wash with 10 CV buffer #5

Elute with a 10 CV gradient (stepwise) of 50 mM NaP pH 7.8, 150 mM NaCl, 10% Glycerol → 50 mM NaP pH 7.8, 1M NaCl, 10% Glycerol

Concentrate in dialysis bag, cover in sucrose, watch to prevent precipitation

Collect fractions and analyze with SDS-PAGE

Dialyze overnight against buffer #7 (storage buffer)

B. Other Experiments Performed, Not Included in this Thesis

Differential Scanning Calorimetry (DSC) of HIV-RT

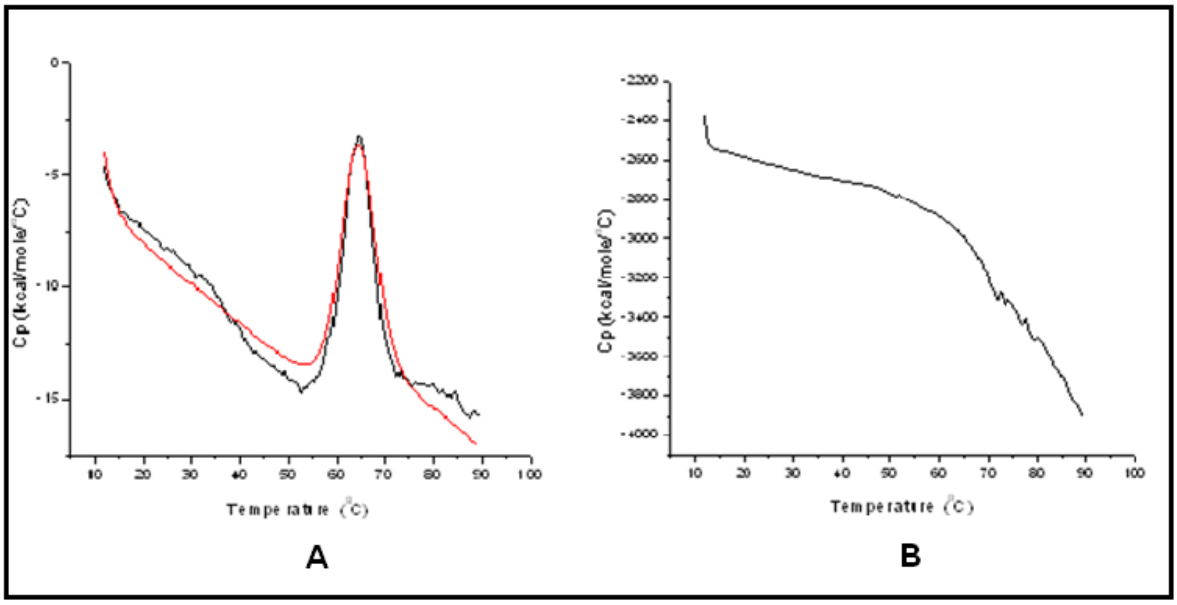

Figure 26. (A) DSC for lysozyme. (B) DSC for HIV-1 RT at 1.5 mg/ml. DSC measures protein unfolding in response to increased temperature. The calorimeter heats two identical cells, one with the protein sample and one with a reference buffer, at the same rate. Since the cell containing the sample typically absorbs more heat than the reference cell, the device provides it with a small amount of heat to balance the temperatures of the two cells. This added temperature (ΔQ) can then be used to find the heat capacity, enthalpy and entropy of the protein denaturation.

DSC was used in this study to assess the thermodynamics of HIV-1 RT unfolding as the protein was heated from 10°C to 90°C. The fact that a discrete peak was not observed may indicate HIV-1 RT precipitation or a lack of subunit dissociation as a result of heating. Continued studies will be done in an attempt to generate a discrete DSC peak for this enzyme.